Near-threshold deuteron photodisintegration: An indirect determination of the Gerasimov-Drell-Hearn sum rule and forward spin polarizability (γ_0) for the deuteron at low energies

M. W. Ahmed,* M. A. Blackston, B. A. Perdue, W. Tornow, and H. R. Weller
Department of Physics, Duke University, Durham, North Carolina 27708, USA and Triangle Universities Nuclear Laboratory, Durham, North Carolina 27708-90308, USA

B. Norum and B. Sawatzky
Department of Physics, University of Virginia, 382 McCormick Road, P. O. Box 400714, Charlottesville, Virginia 22904, USA

R. M. Prior and M. C. Spraker
North Georgia College & State University, Dahlonega, Georgia 30597, USA
(Received 23 July 2007; revised manuscript received 3 December 2007; published 24 April 2008)

It is shown that a measurement of the analyzing power obtained with linearly polarized γ-rays and an unpolarized target can provide an indirect determination of two physical quantities. These are the Gerasimov-Drell-Hearn (GDH) sum rule integrand for the deuteron and the sum rule integrand for the forward spin polarizability (γ_0) near photodisintegration threshold. An analysis of data for the $d(\vec{\gamma}, n)p$ reaction and other experiments is presented. A fit to the world data analyzed in this manner gives a GDH integral value of -603 ± 43 μb between the photodisintegration threshold and 6 MeV. This result is the first confirmation of the large contribution of the ${}^1S_0(M1)$ transition predicted for the deuteron near photodisintegration threshold. In addition, a sum rule value of 3.75±0.18 fm^4 for γ_0 is obtained between photodisintegration threshold and 6 MeV. This is a first indirect confirmation of the leading-order effective field theory prediction for the forward spin-polarizability of the deuteron.

DOI: 10.1103/PhysRevC.77.044005 PACS number(s): 25.20.Lj, 13.60.Hb, 13.60.Le, 27.10.+h

I. INTRODUCTION

The Gerasimov-Drell-Hearn (GDH) sum rule and the sum rule for the forward spin polarizability are both a measure of the spin response of any compound system to photon scattering. These sum rules are a consequence of dispersion relations applied to the forward Compton scattering amplitude. In a low-energy expansion of the forward Compton scattering amplitude, using Lorentz and gauge invariance, the spin-flip part of the expansion can be expressed in odd powers of the photon energy (ω). For the case of the deuteron, the forward scattering amplitude (f_1) can be expanded as [1,2]

$$f_1 = \frac{-\alpha_{em}\kappa^2}{4S^2M^2}\omega + 2\gamma_0\omega^3 + \cdots, \tag{1}$$

where α_{em} is the fine structure constant, and κ is the anomalous magnetic moment of the target with ground state mass M, and spin S. The quantity γ_0 defines the forward spin-polarizability. Using crossing symmetry, unitarity, an unsubtracted dispersion relation and the optical theorem, the first term in the forward Compton scattering amplitude yields the GDH sum rule. This sum rule relates the helicity dependent photoabsorption cross-section difference to the anomalous magnetic moment of the target and states that

$$I^{\mathrm{GDH}} = \int_{\omega_{\mathrm{th}}}^{\infty} (\sigma_P(\omega) - \sigma_A(\omega))\frac{d\omega}{\omega} = 4\pi^2 e^2 \frac{\kappa^2}{M^2} S\,, \tag{2}$$

where $\sigma_{P/A}$ is the photoabsorption cross section with photon and target spins parallel/antiparallel, and ω_{th} is the threshold energy for the inelastic process [1]. The second term in Eq. (1) yields the sum rule for the forward spin-polarizability which for the case of the deuteron is given by

$$\gamma_0 = -\frac{1}{8\pi^2}\int_{\omega_{\mathrm{th}}}^{\infty} (\sigma_P(\omega) - \sigma_A(\omega))\frac{d\omega}{\omega^3}. \tag{3}$$

The GDH sum rule is interesting since it relates a static ground state property, the anomalous magnetic moment, to the excitation spectrum of the target. It also indicates that a nonvanishing anomalous magnetic moment is directly related to the internal dynamical structure of the particle. Furthermore, a finite anomalous magnetic moment restricts the energy-weighted integrated photoabsorption cross-section asymmetry to be positive, i.e., the energy weighted cross section with photon and target spins parallel must be greater than the antiparallel cross section over the full integral.

The deuteron has a small anomalous magnetic moment ($\kappa_d = -0.143$ [3]). The measured value for κ_d predicts a GDH value of $I_d^{\mathrm{GDH}} = 0.652$ μb. This value is significantly less than the predicted GDH values for the proton ($I_p^{\mathrm{GDH}} = 204$ μb) and the neutron ($I_n^{\mathrm{GDH}} = 232$ μb).

*Corresponding author. mohammad.ahmed@duke.edu

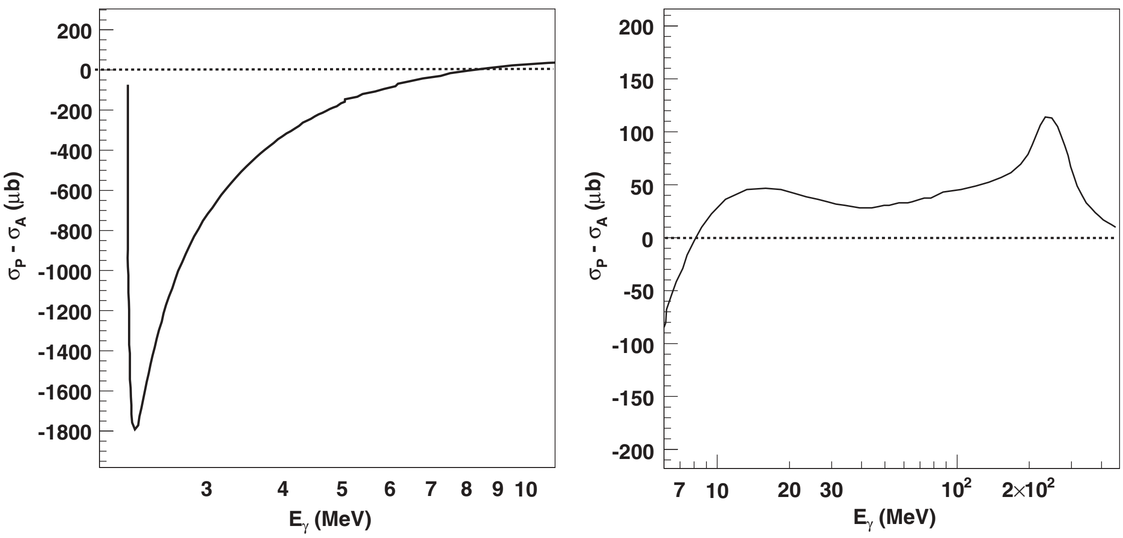

FIG. 1. The GDH sum rule integrand (σ_P-σ_A) for the deuteron. The left figure shows the large, negative near-threshold prediction, and the right figure shows the positive contributions which appear at higher energies.

A theoretical calculation of the GDH integral for the deuteron has been performed by Arenhövel *et al.* [4] up to an energy of 2.2 GeV. This calculation includes the contributions from the photodisintegration channel (up to 0.8 GeV) along with the contributions from the coherent and the incoherent single-pion production channels (up to 1.5 GeV for single pion production and 2.2 GeV for double pion production). Figure 1 shows the predicted results of the GDH integral of the deuteron up to 550 MeV.

The various contributions to the GDH integral are summarized in Table I. As stated in Ref. [4], a very interesting and important result of this theory is the large negative contribution from the photodisintegration channel near the breakup threshold along with a large relativistic contribution below 100 MeV. Note that the integral up to 10 MeV is predicted to be $\sim$$-630$ μb while the value up to pion production threshold is about -530 μb. The largest positive contribution to the GDH integrand arises from the relativistic correction in the energy region up to 100 MeV. As pointed out in the Ref. [5], this large relativistic effect is not surprising since the correct form of the term linear in photon momentum in the low-energy expansion of the Compton amplitude is only obtained if leading order relativistic contributions are included. The present work is the first attempt to test the prediction of the value of the GDH integral between photodisintegration threshold and 10 MeV. Clearly, future studies to verify the positive contribution below 100 MeV will be of great interest.

TABLE I. The GDH integral values from various channels are summarized here [4]. The photodisintegration channel is integrated up to 0.8 GeV, the single pion and eta production channel is integrated up to 1.5 GeV, and the double pion production channel is calculated up to 2.2 GeV.

Process	GDH Integral (μb)
γd $\rightarrow$ np	-381
π production	263
$\pi\pi$ production	159
η production	-14
Total	27

A calculation of the deuteron forward spin polarizability has been performed by Ji *et al.* [2]. The quantity γ_0 has been calculated up to next-to-leading order (NLO) in a pionless effective field theory. The numerical value for the deuteron forward spin polarizability at the leading-order $\gamma_0^{\rm LO}$ is 3.762 fm^4. The NLO term is about 10% of the LO term with $\gamma_0^{\rm NLO} = 0.50$ fm^4. No direct experimental measurement of the deuteron forward spin polarizability exists at present.

A direct determination of the common integrand for the GDH sum rule and the sum rule for forward spin polarizability requires polarized targets and circularly polarized gamma-ray beams. This measurement will be possible at the High-Intensity γ-Ray Source (HIγS)[1] from breakup threshold up to photopion-production energies once the current upgrades are completed. Meanwhile, a number of photodisintegration experiments on the deuteron using linearly polarized gamma rays and unpolarized targets have been performed [6–9]. These experiments covered a range of gamma-ray energies between 2.39 and 16 MeV. The focus of the majority of these experiments was to measure the photon asymmetry of the reaction. The asymmetry ($\Sigma(\theta)$) is given by

$$\Sigma(\theta) = \frac{1}{f}\frac{\sigma(\theta,\phi=0^\circ) - \sigma(\theta,\phi=90^\circ)}{\sigma(\theta,\phi=0^\circ) + \sigma(\theta,\phi=90^\circ)}\,, \qquad (4)$$

where θ is the polar angle and ϕ is the azimuthal angle. The factor f is the fraction of linear polarization in the beam which is taken to be 1.0$\pm$0.02 in the case of the γ-ray beam at HIγS [10]. Using the formalism of Refs. [5,11]

[1]HIGS website http://higs.tunl.duke.edu/; TUNL Web Site http://www.tunl.duke.edu/.

and low-energy approximations argued in Refs. [6,12,13], the photodisintegration cross section for linearly polarized beam and unpolarized target can be written in terms of an $M1$ (S-wave) and an $E1$ (P-wave) matrix element as

$$\sigma(\theta,\phi) = \frac{\lambda\!\!\!^{-2}}{6}\left[\frac{1}{4}|S|^2 + \frac{27}{8}|P|^2\sin^2\theta(1+\cos 2\phi)\right], \quad (5)$$

with

$$\sigma_{\rm total} = \frac{\pi\lambda^2}{6}[|S|^2 + 9|P|^2], \quad (6)$$
$$= \sigma(M1) + \sigma(E1), \quad (7)$$

where S represents the amplitude for the absorption of $M1$ radiation followed by emission of S-wave neutrons while P corresponds to $E1$ absorption followed by P-wave neutrons. The photon asymmetry is then simply

$$\Sigma(\theta) = \frac{\frac{27}{8}|P|^2\sin^2\theta}{\frac{1}{4}|S|^2 + \frac{27}{8}|P|^2\sin^2\theta}. \quad (8)$$

If there is no $M1$ strength in the transition, the theoretical asymmetry would be identical to 1.0 at all angles. Therefore, any asymmetry measured to be less than 1.0, apart from the experimental corrections, would be due to an $M1$ contribution to the cross section. Hence, a photon asymmetry measurement is a direct measurement of the relative strength of the $M1$ S-wave amplitude.

The formalism of Ref. [14] can be used to write the integrand in terms of the contributing transition matrix elements (TMEs). Since we expect only $l = 0, 1, 2$ (S, P, and D waves) in the outgoing n-p channel at very low energies, we obtain

$$\begin{aligned}\sigma_P - \sigma_A = \frac{\pi\lambda\!\!\!^{-2}}{2}\Big[&-|M1(^1S_0)|^2 - |E1(^3P_0)|^2 \\ &-\frac{3}{2}|E1(^3P_1)|^2 + \frac{5}{2}|E1(^3P_2)|^2 - \frac{3}{2}|E2(^3D_1)|^2 \\ &-\frac{5}{6}|E2(^3D_2)|^2 + \frac{7}{3}|E2(^3D_3)|^2\Big],\end{aligned} \quad (9)$$

where the notation $(L_P)^{(2S+1)}l_J$ specifies the S (spin), l (orbital angular momentum), and J (total angular momentum) value of the outgoing n-p channel and L_P specifies the multipolarity (L) and mode (P) of the incoming γ ray. In obtaining this expression we are neglecting the $M1(^3S_1)$, $E1(^1P_1)$, and $E2(^1D_2)$ terms, which are expected to be negligibly small (see Ref. [6]). If splittings of the P- and D-waves are ignored so that the three P-wave amplitudes are taken to be equal to each other and the same for the three D-wave amplitudes, then only the $M1(^1S_0)$ term contributes. In this simplified form the integrand becomes

$$\sigma_P - \sigma_A = \frac{\pi\lambda^2}{2}[-|M1(^1S_0)|^2]$$
$$= -3\sigma(M1). \quad (10)$$

This result indicates that a measurement of the $M1$ cross section in a photodisintegration experiment is an indirect determination of the GDH sum rule and the forward spin polarizability integrand for the deuteron at low energies.

As an example of these indirect measurements, this paper reports the results of an experiment which measured $\sigma(M1)$ at three energies: 2.44, 2.60, and 2.72 MeV at HIγS. An analysis of data from other photodisintegration experiments at HIγS has also been performed in order to extract information on the GDH and forward spin polarizability integrands below 10 MeV. Additional results can be obtained from previously measured polarized neutron capture on proton data as well as unpolarized photodisintegration reaction studies which measured the outgoing neutron polarization. This is the first instance of an experimental evaluation of the GDH sum rule and the sum rule for the forward spin polarizability integrals for the deuteron below 10 MeV.

II. THE EXPERIMENT

The photon asymmetry of the $d(\vec{\gamma},n)p$ reaction was measured using nearly 100% linearly polarized γ rays at energies of 2.72, 2.60, and 2.44 MeV. The deuteron target was a 1 cm thick and 3.8 cm diameter thin-walled plastic disk filled with D_2O, rotated by 45° with respect to the plane normal to the direction of the beam in both the polar and azimuthal angles. The target was surrounded by four ^{6}Li-doped glass scintillator detectors at a polar angle (θ) of 90° and at azimuthal angles (ϕ) of 0°, 90°, 180°, and 270° with respect to the beam direction.

The scintillator detectors were 6.6% (by weight) doped with Li and enriched to 95% ^{6}Li in order to take advantage of the ^{6}Li$(n,t)^4$He reaction for the production of enhanced light output from low-energy neutrons. These Li-glass detectors were 0.95 cm thick and 5.0 cm in diameter. The response of such detectors to low-energy neutrons ($\leqslant$1 MeV) has been studied in detail [15–19]. The front faces of the detectors were placed 7.5 cm from the target disk.

The γ-ray beam passed through a 2.54 cm diameter Pb collimator before striking the target which produced a beam with $\Delta E/E$ of ~2% at these energies. The typical γ-ray flux on the target was ~10^5 γ/sec. Since γ rays at HIγS are produced via Compton backscattering of laser photons from two electron bunches separated by 179 nsec, a time-of-flight (TOF) technique could be used to identify the neutrons from the $d(\gamma,n)p$ reaction. The TOF was given by the time difference between the signal from the Li-glass detectors and the RF signal of the electron storage ring. Figure 2 shows typical TOF spectra for two detectors, parallel and perpendicular to the polarization plane of the γ-ray beam. The detector assembly was periodically rotated by 90° in the azimuthal angle to correct for detection efficiency differences and other instrumental asymmetries. The number of counts in the neutron TOF peak were obtained by integrating the area of the peak which maximized the signal-to-background ratio. The background counts were estimated by integrating a large time region in the spectrum away from the TOF peak. The photon asymmetry is defined in Eq. (4). In the present case the photon asymmetries were calculated by obtaining ratios of counts of every detector in the *original* and *rotated* positions using the expression

$$\Sigma(90^\circ) = \frac{1-\epsilon}{1+\epsilon}, \quad (11)$$

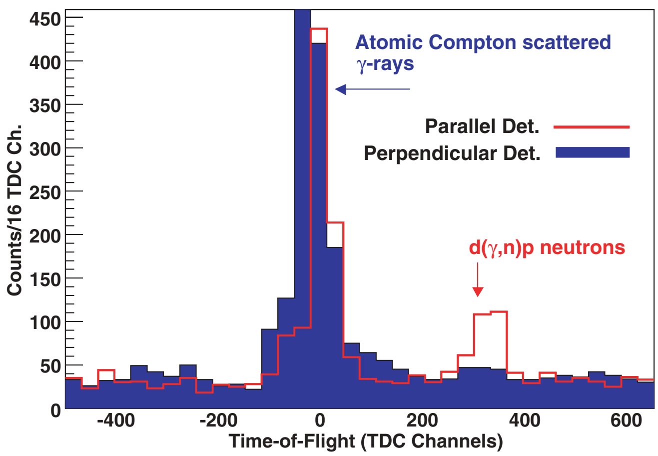

FIG. 2. (Color online) Time-of-Flight (ToF) spectrum from detectors parallel (open) and perpendicular (filled) to the γ-ray polarization axis. The energy of the γ rays was 2.72 MeV.

where

$$\epsilon = \sqrt{\frac{\mathrm{NVO}}{\mathrm{NVR}} \cdot \frac{\mathrm{NHR}}{\mathrm{NHO}}}. \tag{12}$$

In this expression NVO(R) represents the number of counts in the detectors perpendicular (vertical-V) to the polarization axis in the *original* (O) and *rotated* (R) positions, and similarly NHO(R) for the (horizontal-H) parallel case. The numbers of counts were obtained by adjusting the energy cuts as well as summing regions in the TOF spectra until the maximum experimental asymmetry was reached.

At these low energies only $M1$ (S-wave) and $E1$ (P-wave) transitions are expected to contribute to the reaction cross section, as argued in [6] and predicted by potential model and effective field theories [12,20]. In this approximation, the cross section can be written as

$$\sigma(\theta, \phi) = R + \sin^2\theta(1 + \cos 2\phi), \tag{13}$$

which can be related to Eq. (5) by defining the constant R using

$$\tfrac{2}{27}|S|^2 = R|P|^2. \tag{14}$$

The photon asymmetry at $\theta = 90^\circ$ is now simplified to

$$\Sigma(90^\circ) = \frac{1}{1+R}. \tag{15}$$

A Monte Carlo simulation was performed to correct for finite geometry effects and neutron multiple scattering. In this simulation, neutrons of a given energy were distributed uniformly over the physical dimensions of the target volume. The neutron spatial intensity distribution was given by Eq. (13). The parameter R was iterated until the Monte Carlo asymmetry matched the experimental photon asymmetry. The fractional $S(M1)$ contribution to the total cross section was then obtained by using

$$S(M1) = \frac{\frac{9}{4}R}{\frac{9}{4}R + \frac{3}{2}}. \tag{16}$$

The resulting R values and asymmetries are shown in Table II.

TABLE II. The R values and photon asymmetries $\Sigma(90^\circ)$ at various energies.

γ-ray Energy (MeV)	R	$\Sigma(90^\circ)$
2.72	0.127 ± 0.069	0.887 ± 0.054
2.60	0.246 ± 0.123	0.802 ± 0.079
2.44	0.556 ± 0.448	0.642 ± 0.185

In order to extract the absolute $M1$ contribution to the total cross section, the experimentally measured $S(M1)$ was multiplied with the theoretical total photodisintegration cross section. The total photodisintegration cross section given by the EFT calculation of [20] and the potential model calculations of [12] are the same and agree with available data. Either one can be used to normalize the fractional $S(M1)$ contribution to the total cross section. The $M1$ cross section extracted from this fractional $S(M1)$ measurement can then be compared to the predicted $M1$ contribution to the total cross section given by the EFT calculation of [20] or the potential model calculations of [12]. This method provides a way to test the fundamental ingredients of the theory, such as the $M1$ (S-wave) multipole strength. The measured $\sigma(M1)$ are shown in Fig. 3 and compared with the EFT based predictions by [20]. Table III shows the measured $S(M1)$ fraction and resulting $M1$ cross section compared with the predictions from [20].

III. ANALYSIS OF DATA FOR THE INDIRECT DETERMINATION OF THE GDH AND FORWARD SPIN POLARIZABILITY SUM RULE FOR THE DEUTERON

The data on the $M1$ contribution from this experiment and others [6–8,21–24] were analyzed in order to obtain the GDH sum rule integrand using Eq. (10). The data of Refs. [6,7,24] were obtained by photodisintegrating the deuteron and measuring the photon asymmetry ($\Sigma(\theta = 90^\circ$ or 150°). The data set of [8] was obtained using the same technique with full angular coverage between $\theta = 22.5^\circ$ and

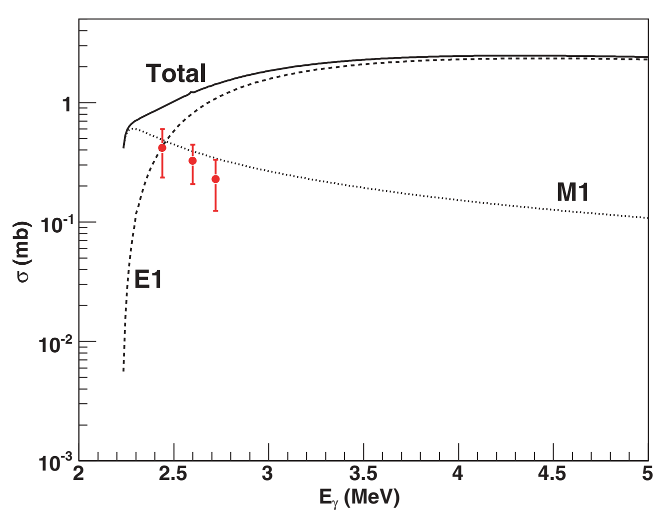

FIG. 3. (Color online) The measured σ(M1) cross section. The three curves are based upon the EFT predictions by [20] of the deuteron photodisintegration cross section.

TABLE III. Measured $S(M1)$ fraction and calculated $M1$ cross section (σ_{M1}) compared to the EFT based predictions by [20].

E_γ (MeV)	$S(M1)$ (Exp.)	$S(M1)$ (Theory) [20]	σ_{M1} (Exp.) (mb)	σ_{M1} (Theory) (mb) [20]
2.72	0.160 ± 0.073	0.230	0.228 ± 0.104	0.340
2.60	0.269 ± 0.098	0.321	0.326 ± 0.119	0.389
2.44	0.454 ± 0.199	0.525	0.418 ± 0.183	0.483

157.5°. In this case, the asymmetry and cross section data as a function of angle were fit using expressions obtained from Ref. [25] in terms of three amplitudes ($M1$, $E1$, and $E2$) and one relative phase ($\phi_P - \phi_D$) in order to obtain $M1$, $E1$, and $E2$ contributions to the total cross section. The relative phase was set equal to the relative phase obtained from an n-p scattering phase shift analysis (∼2°) [26] by invoking Watson's theorem [27]. Since the three triplet ($E1$) P-wave and the three triplet ($E2$) D-wave amplitudes were constrained to be equal, respectively, they did not contribute to the integrand, as shown in Eq. (9).

As previously mentioned, an alternative means of obtaining the same information about the near threshold value of the integrand for the deuteron is from the polarized radiative capture reaction $p(\vec{n}, \gamma)d$. In this case it can be shown that the vector analyzing power at 90° is, for the case in which only $S(M1)$ and $P(E1)$ transition matrix elements contribute, given by

$$A_y(90^\circ) = \frac{3|P||S|\sin(\phi_S - \phi_P)}{1 + \frac{9}{2}P^2}, \qquad (17)$$

with

$$9|P|^2 + |S|^2 = 1.0. \qquad (18)$$

As seen in Eq. (17), the vector analyzing power at 90° arises from the interference between the S- and P-wave amplitudes, and is proportional to the phase difference between these two transition matrix elements. As before the S- to P-wave phase difference can be obtained using the n-p elastic scattering phase shifts. These phase shifts were obtained from the SAID analysis [26]. The value of $\sigma(M1)$ has been obtained from the value of $|S|^2$ (which is proportional to the percentage of the total cross section due to $M1$ radiation) using the total cross section as calculated in Ref. [20]. The polarized n-p capture data from Ref. [22] were analyzed using Eq. (17). The results are shown in Fig. 4.

One additional source of information on the $M1$ strength is the time reversed reaction to the polarized n-p capture study: the unpolarized photodisintegration of the deuteron in which the outgoing neutron polarization is determined. Since time-reversal invariance implies that $A_y(\theta) = P_n(\theta)$, the neutron polarization, $P_n(\theta)$, can be written in an expression which is identical to Eq. (17). Data from [21–23] were analyzed to obtain the relative S strength using Eqs. (17) and (18), and the resulting values were converted to an absolute $\sigma(M1)$ cross section using the theoretical values of the total cross section as in the case of the n-p capture analysis. These results are also shown in Fig. 4.

Another data point is also available as a result of the fact that the thermal n-p capture cross section ($E_n \sim 0.025$ eV) is well measured. The value of this cross section is 332 ± 0.60 mb [28], and is known to be a pure $M1$ cross section. In order to include this in the results shown in Fig. 4, we simply detail balance this cross section, then convert it to σ_P-σ_A using the fact that this is equal to $-3\sigma(M1)$. The result is that for $E_\gamma = 2.225$ MeV, σ_P-$\sigma_A = -1.641 \pm 0.0031$ μb. This point is also shown in Fig. 4.

The results of all of the above extractions of σ_P-σ_A are summarized in Fig. 4. Recall that the basic assumptions made to obtain these results are that the photodisintegration of the deuteron at these energies can be described using $M1$ (with outgoing S-waves), $E1$ (with outgoing P-waves) and $E2$ (with outgoing D-waves). In addition, we have assumed that there is no splitting in the triplet $E1$ P-wave amplitudes and, likewise, in the triplet $E2$ D-wave amplitudes.

The theoretical predictions of [4] are also shown in Fig. 4 as the dashed line. We also show the result from this calculation which is obtained using the approximation σ_P-$\sigma_A = -3\sigma(M1)$. As can be seen in Fig. 4, these two results are in excellent agreement below $E_\gamma \sim 3.5$ MeV, but begin to separate above this energy, with a significant separation showing up at around 4 MeV and above. This is understood as being the result of a contribution to σ_P-σ_A arising from the triplet P- and D-wave matrix elements as the energy increases. All of the data points shown in Fig. 4 were obtained under the assumption that there is no contribution from P- and D-wave splittings. The difference in the two theory curves gives an indication of the size of the effect this approximation could have on these higher energy results and indicates why accurate

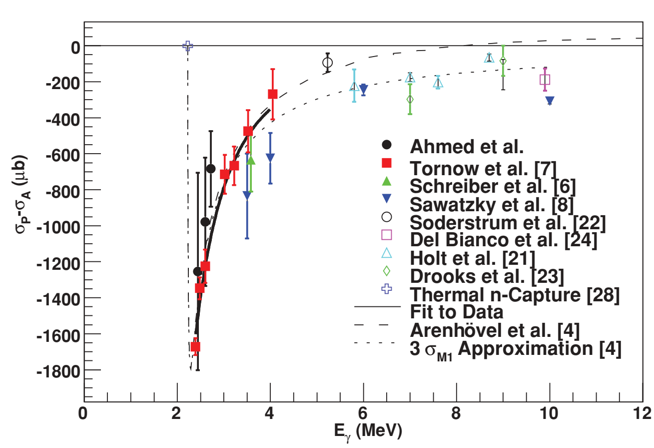

FIG. 4. (Color online) The prediction for the GDH and forward spin polarizability sum rule integrand and indirect measurements.

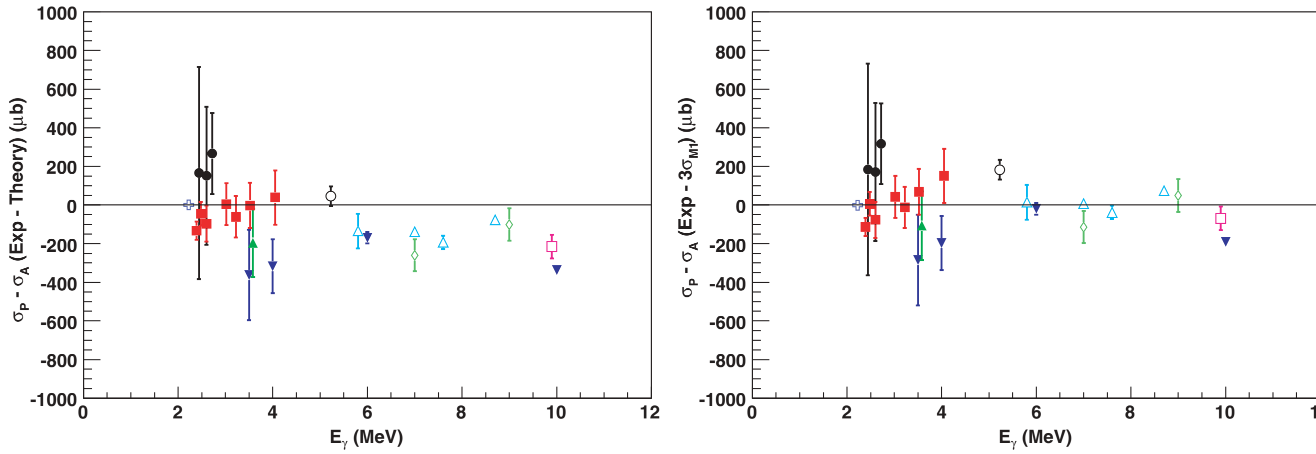

FIG. 5. (Color online) The plot on the left shows the (σ_P-σ_A)(Exp-Theory) and the plot on the right shows the (σ_P-σ_A)(Exp-3σ_{M1}). The legend is the same as Fig. 4.

results will require direct measurements of the GDH integrand using polarized beam and polarized target.

In examining Fig. 4, several discrepancies are apparent and deserve additional comments. First, the result obtained from Ref. [22] (Soderstrum *et al.*) at 5.23 MeV appears significantly higher than the neighboring point from Ref. [21] (Holt *et al.*) at 5.8 MeV. However, when examining the original polarization data, which are the basis of these results, it is seen that the two experimental values differ only by slightly more than one standard deviation. Therefore, we do not consider this difference to be statistically significant.

Another discrepancy is seen near 10 MeV between the result of Ref. [24] (Del Bianco *et al.*) and Ref. [8] (Sawatzky *et al.*). In this case, the data of [24] consisted only of a $\Sigma(90°)$ data point, while those of Ref. [8] were a full angular distribution of $\Sigma(\theta)$. Although the $\Sigma(90°)$ values of both experiments agreed within error, the full angular distribution data set of Ref. [8] allowed for an extraction of the $M1$(S-wave) strength using a fit which included $E1$, $M1$, and $E2$ terms (although with no P- and D-wave splittings), resulting in a larger $M1$ strength. The neglect of $E2$ (D-waves) at higher energies is certainly less justified than it is at lower energies and is the main reason for the discrepancy in the two highest energy points. This behavior can be seen more clearly in Fig. 5 where we have plotted the difference between the experimental values and the full theory as well as with the $3\sigma_{M1}$ prediction.

The full theory, when integrated over energy from threshold to $E_\gamma = 10$ MeV using Eq. (2), predicts a value of -634 μb. The theory also indicates that the value of this integral up to pion threshold is -520 μb. A positive contribution (theoretically arising from a relativistic contribution) between 10 MeV and pion-threshold must be responsible for this reduced value, but remains to be experimentally verified.

In order to extract an experimental value for the GDH and the forward spin polarizability integrals from the results of Fig. 4 a fit was performed on the data of Fig. 4. The functional form of our fit was taken to be Lorentzian. A Lorentzian, parametrized by amplitude, width, and centroid, was used to fit the data by use of the minimization routine MINUIT [29]. Since the S-wave only approximation breaks down as the energy increases, the fit was limited to data below 4 MeV. The results of this procedure produced the solid curve shown in Fig 4. The GDH integral of this function for energy between the photodisintegration threshold and 6 MeV was found to be -603 ± 43 μb. This experimental value is in agreement with the theoretical value of -627 for the GDH sum rule integrated over the same energy range and a value of -662 obtained from the $-3\sigma_{M1}$ approximation. The forward spin polarizability integral of this function from threshold to 6 MeV was found to be 3.75$\pm$0.18 fm^4. This result agrees with the result of the leading order calculation ($\gamma_0^{\rm LO} = 3.762$ fm^4) but is 3σ from the result including the NLO contribution ($\gamma_0^{\rm LO+NLO} = 4.262$ fm^4) [2]. This difference probably arises mainly from the truncation in the integration of the experimental data. A running integral of γ_0 as a function of energy was calculated using the σ_P-σ_A predictions from Arenhövel *et al.* [12]. The result is shown in Fig. 6 with the theoretical results of [2] and our experimental

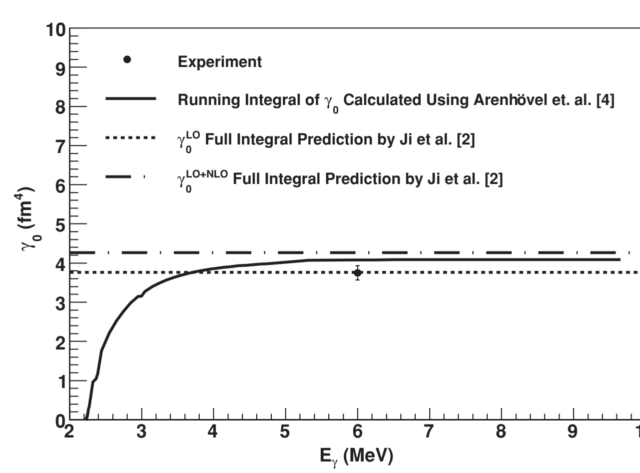

FIG. 6. Running integral of γ_0 calculated using σ_P-σ_A predictions of Arenhövel *et al.* [12]. Also shown are the values of the full integral predictions of Ji *et al.* [2] for $\gamma_0^{\rm LO}$ and $\gamma_0^{\rm LO+NLO}$. The predictions are compared to the experimental result integrated up to 6 MeV.

value. The value of the integral when extended out to 500 MeV (using the predictions of Ref. [12], as shown in Fig. 1) is $\sim$4.1 fm^4. This suggests that the integral is slowly converging to the NLO result of Ref. [2]. At 6 MeV the integral value, as calculated using Ref. [12], is $\sim 1.5\sigma$ from the experimental value. This rather small difference can be attributed to the simplifying assumptions used to extract the data points, as discussed earlier.

IV. SUMMARY

In summary, our indirect determination of the GDH integrand for the deuteron has confirmed the prediction that the $^1S_0$ resonance of the deuteron gives rise to a large negative contribution to the value of the GDH integral below $E_\gamma =$ 10 MeV. The GDH sum rule value we obtain is in agreement with the value predicted by the calculation of Ref. [4]. The forward spin polarizability value which we extract is also the first (indirect) determination of the associated sum rule. The difference between our experimental result and the NLO result of the effective field theory seems likely to be due to the fact that the integral has not converged at out low energies. This conclusion is supported by an explicit integration of the theoretical results of Ref. [12]. This analysis of these data has provided results which constitute the clearest experimental signature of the $^1S_0$ resonance in the deuteron to date. Future direct precision measurements of the GDH and forward spin polarizability integrands at these and higher energies are being planned for the upgraded HIγS facility using circularly polarized γ rays and a polarized deuteron target. Results are expected by late 2008.

ACKNOWLEDGMENTS

The authors would like to thank V. Litvinenko for his support during the production of γ-ray beam at HIγS. We are also thankful to J-W. Chen, G. Rupak, and H. Arenhövel for the theoretical calculations and discussions. This work was supported in part by the US Department of Energy, Office of Nuclear Physics, under grant No. DE-FG02-97ER41033.

[1] S. D. Drell and A. C. Hearn, Phys. Rev. Lett. **16**, 908 (1966); S. B. Gerasimov, Sov. J. Nucl. Phys. **2**, 430 (1966).
[2] X. Ji and Y. Li, Phys. Lett. **B591**, 76 (2004), and references therein.
[3] P. Mohr and B. Taylor, Rev. Mod. Phys. **72**, 351 (2000).
[4] H. Arenhövel *et al.*, Phys. Rev. Lett. **93**, 202301 (2004), and references therein.
[5] H. Arenhövel *et al.*, Few-Body Syst. **3**, 111 (1998), and references therein.
[6] E. C. Schreiber *et al.*, Phys. Rev. C **61**, 061604 (2000).
[7] W. Tornow *et al.*, Phys. Lett. **B574**, 8 (2003).
[8] B. Sawatzky, Ph. D. thesis, Department of Physics, University of Virginia, (2005).
[9] M. A. Blackston, Ph. D. thesis, Physics Department, Duke University (2007).
[10] H. R. Weller and M. W. Ahmed, Mod. Phys. Lett. A **18**, 1569 (2003).
[11] H. R. Weller *et al.*, At. Data Nucl. Tables **50**, 29 (1992).
[12] H. Arenhövel *et al.*, Phys. Lett. **B407**, 1 (1997).
[13] H. Arenhövel *et al.*, Nucl. Phys. **A631**, 612c (1998).
[14] H. R. Weller *et al.*, At. Data Nucl. Tables **58**, 219 (1994).
[15] J. C. Wang *et al.*, Nucl. Sci. Eng. **113**, 77 (1993).
[16] M. Drosg *et al.*, Nucl. Instrum. Methods B **94**, 319 (1994).
[17] S. Sakamoto, Nucl. Instrum. Methods B **299**, 182 (1990).
[18] G. L. Jensen *et al.*, Nucl. Instrum. Methods **220**, 406 (1984).
[19] A. Lajtai *et al.*, Nucl. Instrum. Methods A **293**, 555 (1990).
[20] J-W. Chen and M. J. Savage, Phys. Rev. C **60**, 065205 (1999).
[21] R. J. Holt *et al.*, Phys. Rev. Lett. **50**, 577 (1983).
[22] J. P. Soderstrum *et al.*, Phys. Rev. C **35**, 1246 (1987).
[23] J. Drooks, Ph. D. thesis, Department of Physics, Yale University (1976).
[24] W. Del Bianco *et al.*, Phys. Rev. Lett. **47**, 1118 (1981).
[25] R. G. Seyler and H. R. Weller, Phys. Rev. C **20**, 453 (1979).
[26] Virginia Tech Partial-Wave Analysis Facility (SAID), George Washington University, http://gwdac.phys.gwu.edu/.
[27] L. D. Knutson, Phys. Rev. C **59**, 2152 (1999).
[28] National Nuclear Data Center, Evaluated Nuclear Data File (ENDF), Brookhaven National Laboratory, http://www.nndc.bnl.gov/
[29] F. James, CERN Program Library Long Writeup D506, Version 94.1, CERN Geneva, Switzerland.